

## A Surface Forces Study of DNA Hybridization

Yoon-Kyoung Cho,<sup>\*,†</sup> Sunhee Kim,<sup>†</sup> Geunbae Lim,<sup>†</sup> and Steve Granick<sup>‡</sup>

Biochip Project Team, Samsung Advanced Institute of Technology, Suwon, 440-600, Korea, and Department of Materials Science, University of Illinois, Urbana, Illinois 61801

Received August 30, 2001

We report the first use of a surface forces apparatus to study the hybridization of DNA. We study the regime of very high ionic strength ( $\approx 1$  M) at which commercial DNA chip operations are performed. Using a thiol end-attached single-stranded oligonucleotide, we find that exposure to the complementary strand resulted in larger thickness. In addition, the resistance to small-amplitude shear deformations when opposed to a nonadsorbing surface (mica) increased significantly after hybridization. The thickness at onset of significant shear resistance was, for single-stranded DNA, considerably less than that of hybridized DNA. This could provide a new method to detect DNA hybridization efficiency.

The use of oligonucleotide arrays of DNA to detect the complementary DNA target sequence in a complex DNA target mixture by using the specificity inherent in DNA base pairing<sup>1</sup> is undergoing explosive development because of its usefulness for DNA diagnostics. These hybridization events are also useful for generating nanomechanical cantilever motion,<sup>2</sup> for constructing DNA motors driven by hybridization energy,<sup>3</sup> and for organizing the assembly of colloidal particles.<sup>4</sup> In past work using a surface forces apparatus, force–distance profiles were measured between complementary DNA bases located on opposite surfaces.<sup>5</sup> Atomic force microscopy (AFM) was also applied to measure the forces between complementary strands of DNA<sup>6</sup> and between surface-immobilized DNA when immersed in dilute electrolyte solution.<sup>7</sup> Chemical force microscopy (CFM) was also applied to probe interactions between a peptide nucleic acid (PNA)-functionalized tip and hydrophobic surfaces.<sup>8</sup> Here, for the first time to the best of our knowledge, we study surface forces (compressive as well as shear forces) in the regime of very high ionic strength ( $\approx 1$  M) at which commercial DNA–chip operations are performed. The main novel point is the contrast between static forces and the rate-dependent resistance to small-amplitude shear.

The scheme is sketched in Figure 1. Atomically smooth, step-free sheets of muscovite mica were cleaved according to the usual surface forces apparatus (SFA) technique and brought into crossed-cylinder contact (radius of curvature  $R \approx 2$  cm) inside a surface forces apparatus<sup>9</sup> modified for additional measurements of lateral (shear)

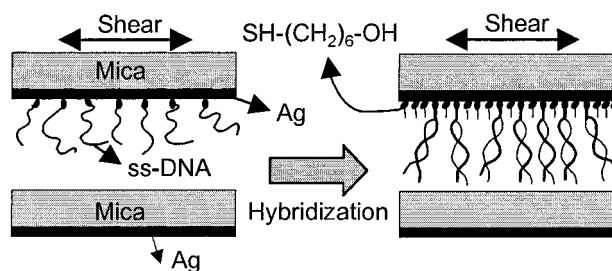


**Figure 1.** Experimental scheme. Thiol-terminated single-stranded DNA, ss-DNA, was allowed to adsorb onto Ag-coated mica, mercaptohexanol was added to impede nonspecific adsorption, and the immobilized films were brought into contact with an opposed sheet of mica to which they did not adsorb.

forces.<sup>10</sup> To take advantage of thiol chemistry for surface immobilization, we sputter-coated a 660 Å thick silver layer onto one of the mica sheets and exposed this to DNA as described below. Surface separation was then measured (in an approach taken previously for adhesion studies<sup>11</sup> and one prior study of force–distance relations<sup>12</sup>) by multiple beam interferometry between this Ag layer and a second Ag layer on the backside of the other mica sheet. A strong van der Waals attraction was observed in air, as indicated by “jumps” into flattened contact from  $\approx 300$  Å separation. The wavelengths of constructive interference at different flattened spots were the same within  $\pm 2$ –4 Å. Despite the roughness of the exposed Ag layer, estimated as 1–2 nm root mean square, relative changes of surface separation appeared to be well-defined. The refractive index of the aqueous gap (DNA in aqueous salt solution) was assumed to be 1.46.<sup>13</sup>

The oligonucleotides, whose sequence was chosen because it is believed to be a part of the Iduronate-2-sulfate (IDS) exon whose mutation is believed medically to be the sequence that causes Hunter syndrome, were purchased from Research Genetics (Huntsville, AL). Thiol-terminated on the 5′ end by an alkanethiol spacer, the sequence was (SH–C<sub>6</sub>–5′–GTT CTT CTC ATC ATC–3′), with molecular weight  $M = 4651$  g mol<sup>−1</sup>. This ss-DNA

\* To whom correspondence should be addressed. Tel.: 82-31-280-8089. Fax: 82-31-280-9357. E-mail: dnachip@samsung.co.kr.

<sup>†</sup> Samsung Advanced Institute of Technology.

<sup>‡</sup> University of Illinois.

(1) Ramsay, G. *Nature Biotechnology* **1998**, *16*, 40.

(2) (a) Fritz, J.; Baller, M. K.; Lang, H. P.; Rothulzen, H.; Vettiger, P.; Meyer, E.; Güntherodt, H.-J.; Gerber, Ch.; Gimzewki, J. K. *Science* **2000**, *288*, 316. (b) Wu, G. H.; Ji, H. F.; Hansen, K.; Thundat, T.; Datar, R.; Cote, R.; Hagan, M. F.; Chakraborty, A. K.; Majumdar, A. *Proc. Natl. Acad. Sci. U.S.A.* **2001**, *98*, 1560.

(3) Yurke, B.; Turberfield, A. J.; Mills, A. P.; Simmel, F. C.; Neumann, J. L. *Nature* **2000**, *406*, 605.

(4) Mirkin, C. A.; Letsinger, R. L.; Mucic, R. C.; Storhoff, J. J. *Nature* **1996**, *382*, 607.

(5) Pincet, F.; Perez, E.; Bryant, G.; Lebeau, L.; Mioskowski, C. *Phys. Rev. Lett.* **1994**, *73*, 2780.

(6) Lee, G. U.; Lisey, L. A.; Colton, R. G. *Science* **1994**, *266*, 771.

(7) Wang, J.; Bard, A. J. *Anal. Chem.* **2001**, *73*, 2207.

(8) Liubashovski, O.; Patolsky, F.; Willner, I. *Langmuir* **2001**, *17*, 5134.

(9) Israelachvili, J. N. *Intermolecular and Surface Forces*, 2nd ed.; Academic Press: New York, 1992.

(10) Granick, S. *Science* **1991**, *253*, 1374.

(11) Quon, R. A.; Vanderlick, T. K. *Langmuir* **2000**, *16*, 3797.

(12) Sheth, S. R.; Efremova, N.; Leckband, D. E. *J. Phys. Chem. B* **2000**, *104*, 7652.

(13) Jordan, C. E.; Frutos, A. G.; Thiel, A. T.; Corn, R. M. *Anal. Chem.* **1997**, *69*, 4939.

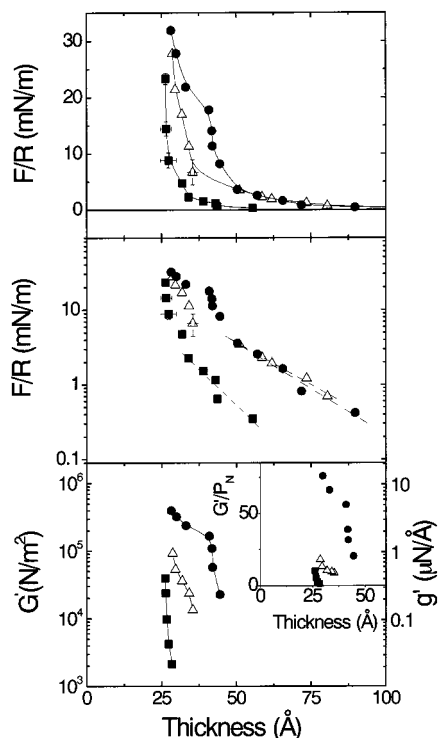


**Figure 2.** Forces in the compressive and shear directions are compared before and after hybridization with the complementary DNA strand: squares, ss-DNA in 1.0 M NaCl; triangles, ss-DNA in 1.0 M NaCl after adding an excess of mercaptohexanol; circles, in 1.0 M NaCl after hybridization. Forces in compression, normalized by the radius of curvature  $R$ , are plotted on a linear scale (top panel) and a semilogarithmic scale (middle panel). The bottom panel compares the shear forces, normalized as described in the text, on a semilogarithmic scale. The inset shows, plotted against surface separation, the dimensionless ratio of shear to compressive force at 1.3 Hz, having normalized both forces by effective area using the Langbein approximation.<sup>9</sup>

was allowed to adsorb onto Ag for 3 h from a concentration of  $1 \mu\text{M}$  in 1 M  $\text{NaH}_2\text{PO}_4$  buffer at pH 4.0. The sample was rinsed with buffer and then water and was then dried with  $\text{N}_2$  gas. In experiments involving a “spacer” to impede physisorption of the DNA, 1 mM mercaptohexanol,  $\text{HS}-(\text{CH}_2)_6\text{OH}$ , was allowed to adsorb for 10 min. Then the sample was rinsed with deionized water and dried in  $\text{N}_2$  gas. For hybridization, the complementary sequence 3'-CAA GAA GAG TAG TAG-5' was exposed to the surface from concentration  $1.5 \mu\text{M}$  in TE buffer (10 mM Tris HCl, 1 mM EDTA, 1 M NaCl) for 2 h at pH = 7.6 and  $40^\circ\text{C}$ . Finally this was rinsed with warm TE buffer, rinsed with deionized water, and dried with  $\text{N}_2$  gas. A drop of 1 M NaCl was added to the dry sample, and measurements were begun.

Control experiments showed that the DNA did not adsorb to untreated mica—as anticipated, because DNA is anionic and the mica surface, in water, also carries negative charges. Therefore the DNA samples were attached strongly by the thiol group in an end-tethered configuration and lacked nonspecific attraction to the opposed mica surface. The experiments were performed at the University of Illinois.

Force–distance profiles at  $25^\circ\text{C}$  are shown in Figure 2. The scales are linear in the top panel and semilogarithmic in the middle panel, and the bottom panel compares to shear forces. For comparison, the contour lengths are estimated as  $77 \text{ \AA}$  for the ss-DNA and  $63 \text{ \AA}$

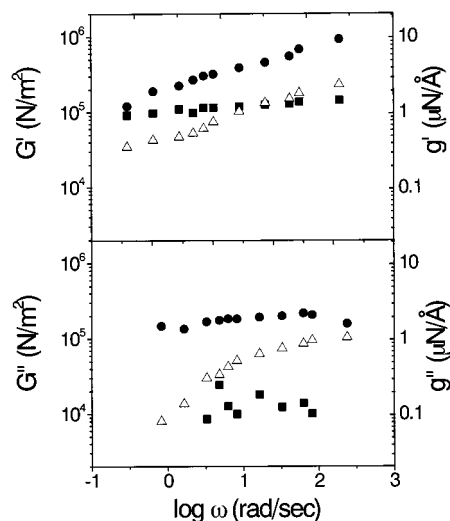


**Figure 3.** Shear forces of ss-DNA and ds-DNA (symbols are same as in Figure 2) are plotted against frequency on log–log scales in measurements performed at  $D = 31 \pm 2 \text{ \AA}$ . On the left-hand ordinate is plotted the effective elastic shear modulus,  $G'$  (top panel), and loss modulus,  $G''$  (bottom panel), forces having been normalized for effective area using the Langbein approximation.<sup>9</sup> Equivalently (without normalization for effective area), on the right-hand ordinate are plotted the elastic and viscous shear force constants.

for the ds-DNA (15 base pairs of length  $4.3 \text{ \AA}$  for ss-DNA<sup>14</sup> and  $3.4 \text{ \AA}$  for ds-DNA, plus mercaptohexane spacer  $12 \text{ \AA}$ <sup>15</sup>). For the thiol-terminated ss-DNA without added mercaptohexanol, one sees that the static forces began at  $43 \pm 2 \text{ \AA}$  and met a “hard wall” at  $26 \pm 2 \text{ \AA}$ . After mercaptohexanol was added, the onset of forces moved out, corroborating conclusions by others that DNA in the former instance adsorbs in a somewhat flattened configuration.<sup>14</sup> In the force–distance profile of the system containing hybridized DNA, one sees that changes were monotonic down to the thickness of  $41 \pm 2 \text{ \AA}$ . This was followed by an abrupt change of thickness, to  $30 \pm 2 \text{ \AA}$ , implying that the rigid ds-DNA changed tilt angle to sustain the large normal pressure. Finally, we note that the onset of measurable shear forces (bottom panel) occurred at decidedly smaller separations than the onset of repulsive forces. The normalization of these shear forces is described below.

To determine the adsorbed amounts, separate interferometric measurements were made of the dry thickness of these samples (dried over nitrogen). For ss-DNA the dry thickness was  $9 \pm 2 \text{ \AA}$ , which implied an adsorbed amount of  $1\text{--}1.5 \text{ mg m}^{-2}$  ( $1.9 \times 10^{13}$  chains  $\text{cm}^{-2}$ ) assuming that the density of DNA was  $1.70 \text{ g cm}^{-3}$ .<sup>16</sup> The estimate implies a mean chain spacing of  $\approx 23 \text{ \AA}$ , the same order of magnitude as the persistence length of  $\approx 10 \text{ \AA}$  measured for ss-DNA of a somewhat different sequence distribution.<sup>13</sup>

How to explain the decay lengths of forces in Figure 2? It is remarkable to see (middle panel of Figure 2) that the compression forces could always be described by a single decay length,  $26 \text{ \AA}$  (ss-DNA),  $40 \text{ \AA}$  (ss-DNA plus mercaptohexanol spacer), and  $40 \text{ \AA}$  (ds-DNA). These numbers are decidedly larger than the Debye length (the Debye length at 1 M NaCl is only  $3 \text{ \AA}$ ), so it would be a mistake

(14) Tinland, B.; Pluen, A.; Sturm, J.; Weill, G., *Macromolecules* **1997**, *30*, 5763.

(15) (a) Levicky, R.; Herne, T. M.; Tarlov, M. J.; Satija, S. K. *J. Am. Chem. Soc.* **1998**, *120*, 9787. (b) Huang, E.; Satjapipat, M.; Han, S.; Zhou, F. *Langmuir* **2001**, *17*, 1215.

(16) Lewin, B. GENES VI; Oxford University Press: New York, 1998.

to seek to fit these curves to the Poisson–Boltzmann equation. We tentatively attribute the force–distance profiles mainly to steric interactions of the end-tethered DNA with the opposed surface. Hydration forces between that polar surface and the polar DNA may also contribute. However, although we have confidence in the force measurements when the compression was large (when relative changes were most meaningful), surface roughness may have contributed at the “tails” of the measured force–distance profiles, when the forces were small, so no quantitative explanation is offered at this time.

We now turn to stiffness in the lateral direction (Figure 3). The amplitudes of deformation were kept small,  $<2 \text{ \AA}$ , to maintain a linear response. With the in-phase (elastic) and the out-of-phase (viscous) responses assigned to sinusoidal excitation at variable frequency, the spectrum of response was quantified. One observes that elastic forces exceeded viscous forces and that the magnitudes increased remarkably after hybridization, presumably because of

enhanced chain stiffness. Even more significantly (see inset in Figure 2), after hybridization the shear forces dominated the compression forces. The large magnitude of this effect suggests that this could provide a method to detect the efficiency of hybridization. Experiments are in progress to test the sensitivity of this characterization method to single-point mutations in the complementary strand.

**Acknowledgment.** We thank Marina Ruths for helpful discussions and Dongkyu Jin for providing us the sequence of DNA samples. This work was supported by the Samsung Corporation (Y.K.C. and S.K.) and by the U.S. Department of Energy, Division of Materials Science under Award No. DEFG02-ER91ER45439, through the Frederick Seitz Materials Research Laboratory at the University of Illinois at Urbana-Champaign (S.G.).

LA0113769